Available online at website: https://journal.bcrec.id/index.php/bcrec

Bulletin of Chemical Reaction Engineering & Catalysis, 20 (3) 2025, 411-427

Original Research Article

Green Synthesis of Silver Nanoparticles using Amomum Subulatum: Characterization and Evaluation of Antioxidant, Antimicrobial, and Catalytic Activities

Sonam Baghel[1], Monika Khurana[1*], Prachi Gupta[2]

[1] *School of Engineering & Technology, Sushant University, Sector-55, Gurugram-122003-Haryana, India.*
[2] *Department of Biotechnology, Government College for Girls, Sec-14, Gurugram-122001-Haryana, India.*

Received: 7th April 2025; Revised: 23th May 2025; Accepted: 24th May 2025
Available online: 17th June 2025; Published regularly: October 2025

Abstract

The seeds extract of Amomum Subulatum commonly known as black cardamom is used for preparing Silver Nanoparticles (AgNps) via green route. The characterization of these nanoparticles was done by UV-visible, Fourier transform Infrared (FTIR) spectroscopy, X-ray diffraction (XRD) and Transmission Electron Microscopy (TEM) techniques. The UV-vis spectra showed sharp absorption maximum at 432 nm that confirmed that AgNPs were synthesized successfully. The TEM measurements indicated that AgNps are mostly spherical with a few having hexagonal and trigonal shapes with size range of 13-21 nm. Dynamic Light Scattering (DLS) confirmed the stability of AgNps having negative zeta potential. XRD confirmed the mono-crystallinity of the prepared AgNps. A significant zone of inhibition is observed by these nanoparticles against gram positive and gram-negative bacteria. These nanoparticles exhibit a significant catalytic activity with respect of 4-nitrophenol (4-NP). The synthesized AgNps act as a catalyst and degraded the organic dyes, Methylene Blue (MB) and Methylene Orange (MO) by Sodium borohydride ($NaBH_4$) as confirmed by UV-vis spectroscopy.

Keywords: Green Synthesis; Silver nanoparticles; Black cardamom; Catalytic activity; Dye degradation; Antibacterial activity

How to Cite: Baghel, S., Khurana, M., Gupta, P. (2025). Characterization of Silver Nanoparticles Prepared via Green Synthesis from Amomum Subulatum: Investigation of its Antioxidant, Antimicrobial and Catalytic Properties in Dye Degradation. *Bulletin of Chemical Reaction Engineering & Catalysis*, 20 (3), 411-427. (doi: 10.9767/bcrec.20374)

Permalink/DOI: https://doi.org/10.9767/bcrec.20374

1. Introduction

Nanoparticles exhibit unique properties as compared to their bulk counterparts due to differences in particle characteristics, such as size, dispersion, and shape [1]. These metal nanoparticles have distinctive optical features because of their high surface area to volume ratio. The rapidly developing field of plasmonic has made intelligent and widespread use of these optical features [2,3]. Additionally, According to several studies; these nanoparticles also exhibit catalytic [4–11], and electrochemical applications [12]. In general, silver nanoparticles are synthesized using various chemicals as stabilizing and reducing agents, the chemical reduction method posing a serious risk to humans and the environment. In recent years, the manufacture of nanoparticles through green methods using plant extracts has replaced the use of harmful chemicals [13]. Green nanoparticle synthesis is a fascinating field in material science since it is less toxic, biocompatible and easy to functionalize with biomolecules and it doesn't need the use of dangerous chemicals. Despite their low yield percentage, green produced metal nanoparticles are interesting prospects for future study fields, such as biosensors, nanodrugs and bio-based nanoelectronics. Since it has a varied range of applications in bioscience, green production of

* Corresponding Author.
Email: monikakhurana@sushantuniversity.edu.in (M. Khurana)

noble metal nanoparticles is getting a lot of focus in the chemical and material science fields.

Metal nanostructures are used in many different fields in the biological and medical industries [14] in biomedical research, they can be employed for medication delivery, biosensing, bio-imaging and biomolecular recognition. Integration of green chemistry principle to nanotechnology is key issue in nanoscience research. There is growing need for environment friendly green nanoparticles (size 1-100 nm) that do not use toxic chemicals and avoid adverse effect [15]. Fungi, bacteria, enzymes, and plant extracts are commonly used in the green manufacture of silver nanoparticles (AgNps). Few plants used for the synthesis of AgNps are Malabar Nut [16], Pineapple [17], Kalmegh [18], Tulsi [19], Neem [20], Onion [21], Shatavari [22], Nagarmoth [23], Shalparni [24]. Silver nanoparticles are well-known for their antibacterial [20,21,25–28], catalytic and optical capabilities, but due to high demand and scarcity, they are exceedingly expensive and difficult to obtain [29]. Silver nanoparticles are considered biocompatible, in which there is the possibility that a chemical reduction method results in toxic chemical species [30] being adsorbing onto their surface, so they must be removed in an additional step. As a result, medical applications may experience some adverse effects. So, there is an urgent demand to develop environmentally safe nanoparticles.

Nano-silver has been shown in research and publications to have negative impacts on persons and the environment. The green technique, on the other hand, allows for harmful chemical-free and environmentally friendly AgNps synthesis [31]. AgNps are inert, they have better biocompatibility [32], which is important in most biological applications like they have the capacity to be easily conjugated with biological molecules[33]. The size and morphology of AgNps determine their activity, which is influenced by the preparation, solvent type, concentration, reducing agent and temperature. The shape, size, and surface properties of AgNps made them ideal for biosensors [34,35], hyperthermia therapy [36], delivery systems for therapeutic drugs, genetic materials, antifungal effect, anti-tumorigenic ability [37] and anti-coagulative activity [38].

Because of their antimicrobial capabilities, such nanoparticles are used in variety of daily items e.g. cosmetics, toothpaste, deodorants. A substantial contribution has been made by AgNps to agriculture and technology, purification systems, and humidifier. They used in detecting and treating plant diseases and lowering nutrient leaching to increase crop yield. They're also used in solar and oxide batteries to store energy. Black cardamom is the dried fruit of a perennial herbaceous plant in the family Zingiberaceae [39]. One of the foremost commercial crops of the Eastern Himalayan Region and is grown in marshy areas near streams, across hills. This spice is well-known for its distinctive taste and aroma and is commonly used to flavor dishes from the Himalayan region, which involves Nepal, Bhutan, and India. According to the Ayurvedic and Unani systems of medicine, black cardamom is widely used in ethnomedicine. Traditional uses of this herb include treating coughs, lung congestion, pain, stomach disorders, and many other ailments. Due to advent of modern phyto-analytical and pharmacological techniques and the popularity of natural products-based medicine, the therapeutic use of this ancient spice is gaining a new dimension.

Recent studies reported that Black cardamom contains high levels of polyphenols, which may assist in reducing and stabilizing nanoparticles [13,40,41]. These bioactive compounds provide antioxidant, antimicrobial (antibacterial [38,27] and antifungal [42]), analgesic [43], anti-inflammatory, antiulcer [44], cardio-adaptogen, and hypolipidemic properties. A common uses of black cardamom (BC) is in Indian cuisine, beverages, mouth fresheners, and traditional medicine. Its antioxidant action has been shown to provide health benefits. Studies have also reported that black cardamom may have anti-inflammatory [45], anti-diabetic [14], and anti-cancer properties [46]. It is a versatile spice with many potential health benefits. Its waste peels used in removing Cd(II) from water [47] and Congo red from water [48]. In our synthesis protocols, BC is used as a reducing agent. In this study, we establish a new, eco-compatible, and green AgNps synthesis from Ag(II) salts using extract from black cardamom as a natural reducer.

2.Material and Methods

2.1 Materials

The Chemicals Silver Nitrate, Sodium Borohydride, p-nitrophenol, Methylene Blue and Methyl orange were purchased from Sigma Aldrich Chemicals private limited. DPPH, Nutrient Agar and Disc were purchased from Himedia Laboratories Private Limited. Gram-positive bacteria (*Bacillus subtilis* MTCC 441, *Staphylococcus aureus* MTCC 3160), and Gram-negative bacteria (*Pseudomonas aeruginosa* MTCC 647, *Escherichia coli* MTCC 16521) were procured from GJU university, Hisar, Haryana, India. All the reagents and chemicals used in the entire study were of analytical grade. All experiments were conducted using Milli Q and Double Distilled water. The chemicals were not further purified before being use. Black Cardamom was obtained from local supermarket. Plant authenticity of black cardamom has been done by RHMD, CSIR-NIScPR, New Delhi, India.

2.2 Preparation of Seed Extract and Biosynthesis of Silver Nanoparticles (AgNps)

Black cardamom seeds were used to prepare plant extract. 5 g seeds of black cardamom were given a two-time washing with double distilled water to get free from any attached foreign particles, then they were dried in an oven at 50 ^{0}C for 30 minutes and then crushed it into a fine powder using pestle and mortar. 5 g of freshly prepared dry seed powder was suspended in 100 mL of distilled water [49] and boiled at 75 ^{0}C for 1.5 hours on magnetic stirrer [26]. The prepared plant extract was filtered using whatmann filter paper no. 1, keeping supernatant for further experimental use at 4 ^{0}C.

0.14 g of $AgNO_3$ was taken on watch glass and dissolved it in 40 mL of Milli-Q water [49] and then 10 mL of plant extract was added to it then the mixture was heated at 75 ^{0}C for 30 minutes on magnetic stirrer, change in the color from pale yellow to dark brown indicated the formation of AgNps [26]. The resulting Silver nanoparticles are stabilized over 2 months [5].

2.3 Characterization of Green Synthesized Silver Nanoparticles

2.3.1 UV – Vis spectroscopy

An ultraviolet-visible spectrophotometer (Shimadzu UV-1800) was used to confirm the formation of Silver nanoparticles against Milli-Q water as a blank. In this experiment, the reaction mixture absorbance was measured between 300 and 700 nm. For recording the spectra, 1 mL of prepared colloidal AgNps solution was collected in a cuvette and diluted by 2 mL Milli-Q water.

2.3.2 TEM analysis of silver nanoparticles

In depth analysis of morphology, size, distribution, and aggregation of AgNps were performed by High resolution transmission electron microscopy (TALOS 200 kV). The synthesized AgNps colloidal solution were centrifuged at 10,000 rpm at a temperature of 25 ^{0}C for 15 minutes. The supernatant was separated for TEM measurements. Before the experiment, the AgNps were sonicated for proper dispersal, then 10 µL was pipetted out on carbon coated TEM grid to make a thin film. Then that grid was placed in a hot air oven at 50 ^{0}C for 30 minutes in order to ensure its dryness. Analyses were conducted at a variety of magnifications to determine the size of nanoparticles.

2.3.3 XRD study

X-ray diffractometer (Bruker D8 Discover) equipped with Cu-Kα radiation source and nickel monochromator filter was used for the measurement. The spectra was taken in the range of 20-80^0 of 2θ at the scanning rate of 20 degrees per minute [50]. Average particle size was determined by Debye- Scherer equation:

$$D = K\lambda/(\beta \cos \theta) \quad (1)$$

It consists of Scherer's constant K, whose value ranges between 0.9 and 1, and is commonly known as the crystallite-shape factor. D is the average crystallite size in the direction perpendicular to the lattice planes, λ is the wavelength of the X-rays source used in XRD, β is the width (full-width at half-maximum) of the X-ray diffraction peak in radians and θ is the Bragg angle [50]. The numerical factor K depends not only on the shape of crystallites, but also on the definitions of the average size of crystallites. In absence of detailed information of size, K value approximately taken as 0.9. According to Scherer; this equation can be applied to average size 100 to 200 nm [51].

2.3.4 Fourier-Transform Infrared Spectroscopy (FT-IR)

Infrared spectra of the plant extract were recorded using FTIR spectrophotometers (Shimadzu IR affinity 1S) for characterization of silver nanoparticle surface structure in wavelength ranges 4000-400 cm^{-1} prior to and after reduction [50]. As per the studies done by Wang *et al*. on the pharmacological composition of black cardamom, and they show that the primary components are 1,8-cineole (65%), α-Pinene (0.85%), and α-Terpineol (7.92%) out of the 40 discovered chemicals [52]. FTIR spectra of plant extract and the synthesized AgNps were recorded [53].

Size and surface charge by DLS -The zeta potential and hydrodynamic size of the prepared AgNps were determined using a Zetasizer Nano ZS, Malvern Instruments Ltd. Colloidal AgNps were centrifuged at 10000 rpm for 10 minutes and then supernatant was collected for DLS measurements. One ml sample of prepared AgNps was taken for DLS studies.

2.4 Applications of AgNps: Catalytic Efficiency of Silver Nanoparticles

2.4.1 Conversion of p-nitrophenol into p-aminophenol

Industrial wastes are one of the main components of causing water pollution. Dye industry and agrochemical industries discard p-nitro phenol which is very harmful and highly stable compound but it can be easily transformed into a convenient compound p-amino phenol, which further can be used in the preparation of other important compounds in pharmaceutical industry. In this report, the catalytic reduction takes place by using AgNps and this conversion

was observed by UV spectrophotometer using Milli-Q water as blank. A freshly prepared 1 mL of 15 mM $NaBH_4$ [54] solution was added to 1.9 mL of 0.2 mM p-nitrophenol solution. The immediate color change was detected and quantitatively measured by UV-Vis spectroscopy. Subsequently, 10 µL of 1.0 mg/mL AgNps [9] were added and the recorded the progress of the reaction by scanning from 200 to 600 nm spectrophotometrically at 2 minutes time interval and graphs were plotted between absorbance and wavelength using origin [55]. A control experiment was also conducted using $NaBH_4$ and p-nitrophenol, as well as silver nanoparticles and p-nitrophenol. Experiments were performed in triplicates. In this reaction, the rate constant was determined by the change in absorbance at 400 nm over time.

2.4.2 Reduction/degradation of organic dyes

Organic Dyes lead to color contamination of various water bodies. So, act as toxic substances. There are two characteristic UV-Vis absorption peaks in methylene blue, one at 664 nm, which is caused by MB monomer [56] and another shoulder peak at 612 nm results from MB dimers [57]. The first peak originates from the conjugation of two dimethylamine substituted aromatic groups via MB's sulfur and nitrogen atoms. As a result of the substitution of benzene in the spectrum, two additional bands appear in the UV region near 245 and 290 nm [56]. To study degradation of organic dyes, 10 mg/L solutions of Methylene blue (MB) and methyl orange (MO) were prepared in Milli-Q water. To study dye degradation, 2.5 mL of MB and MO were mixed with 100 µL of 0.2 M $NaBH_4$ solution and 20 µL of 1.0 mg/mL AgNps. The degradation of dyes was monitored by measuring the absorbance from 200 to 800 nm using UV-Vis spectrophotometer at 2 min time intervals and graphs were plotted between absorbance and wavelength using origin. Control experiment was also performed using a mixture of dye solution and Additionally, $NaBH_4$ was performed in order to provide a comparison [55]. Experiments were performed in triplicates.

2.4.3 Antibacterial efficacy of AgNps

The anti-bacterial efficacy of AgNps were determined against four bacterial strains including Gram-positive bacteria (*Bacillus subtilis* MTCC 441, *Staphylococcus aureus* MTCC 3160), and Gram-negative bacteria (*Pseudomonas aeruginosa* MTCC 647*, Escherichia coli* MTCC 16521) on nutrient agar plates, using disc diffusion methods. All bacterial strains were obtained from Department of Bio and Nanotechonolgy, GJU, Hisar, Haryana. A spread-nutrient agar plate of fresh overnight culture was prepared using sterile spreader under Laminar Air Flow hood. For evenly distribution on the agar plate 50 µL of overnight culture was used. The plates were well labelled for different bacterial strains. The AgNps solution is infused with different concentrations of biosynthesized AgNps onto a sterile Whatman No 1 paper disc of 6 mm in size. Then the discs were mildly pressed on nutrient agar plates seeded with 50 µL bacterial culture. For the control, Streptomycin (10 µg/disc) was maintained on each plate. The plates were incubated at 37 °C for 24 h in sterile condition. Next day, the plates were removed and the diameter of zone of inhibition (ZoI) was measured for each concentration of biosynthesized AgNps. Anti-bacterial efficacy of AgNps of each bacterial strain were performed in triplicates. The average diameter of each concentration's ZoI was tabulated.

2.4.4 In vitro determination of antioxidant activity of Biosynthesized AgNps

Biosynthesized AgNps were examined for antioxidant activity using 1,1-Diphenyl-2-picrylhydrazyl radical (DPPH), which is a stable free radical molecule [58]. 0.1 mM DPPH having a characteristic absorbance maximum at 517 nm (deep violet). DPPH radical absorbance maxima changes by Scavenging of DPPH radical to DPPH by antioxidants, i.e. decolorized it to yellow. As a result of its convenience and ease of use, the DPPH radical scavenging assay is widely used to assess free radical scavenging.

For this, different volumes of biosynthesized AgNps (0, 100, 500, 1000, 1500 µg/mL) [58] were used and its volume is to be made 2 mL by adding methanol and then 1 mL of DPPH was added then vortex it and incubate in dark for 30 min. For control, 2 mL methanol and 1 mL DPPH was taken. The DPPH radical scavenging activity in terms of percentage inhibition of DPPH radical was calculated according to the following equation [59]:

$$DPPH\ radical\ scavenging\ activity\ (\%) = \{(Abs_{517\ control} - Abs_{517\ sample} / Abs_{517\ control})\} \times 100 \quad (2)$$

where, $Abs_{517\ control}$ is the absorbance of the blank and $Abs_{517\ sample}$ is the absorbance of the AgNps at different concentrations.

3. Result and Discussion

3.1 Characterization of Silver Nanoparticles

3.1.1 UV spectroscopy

The UV-Visible spectroscopy provides important information about the stability and formation of metal nanoparticles. In the UV-Vis range, nanoparticle solutions exhibit absorption bands that are caused by oscillations in surface plasmons of Ag metal electrons, which gives

information regarding the nanoparticle shape and size [60]. The synthesized silver nanoparticles are immediately spectroscopically studied for further study. The spectrum was recorded using 1 mL of reaction mixture diluted in 3 mL of double distilled water or Milli-Q water. These recorded spectra have been shown in Figure 1. It has been observed that the absorption maxima of silver nanoparticles are located at a wavelength of 432 nanometers indicates the formation of AgNps. There are no peaks in the surface plasmon band between 450 and 600 nm, indicating that nanoparticles are not aggregating.

Researchers have reported that the properties of metal nanoparticles vary with the position and intensity of the surface plasmon peak [61]. Black Cardamom seed extract contains a variety of phytochemicals, including flavonoids and phenolic compounds. These phytochemicals act as both a stabilizing and reducing agent during AgNps production. When the plant extract was mixed with $AgNO_3$ solution, the Ag ions were reduced to Ag atoms, which then bonded to produce nano-level particles. Phytochemicals also create a coating on AgNps, protecting them from coalescence. The fact is that the surface plasmon resonance (SPR) band of Silver nanoparticles does not vary significantly in position even after 2 months of storage at ambient temperature (Figure 1c) which demonstrates the potential of phytochemicals to stabilize the nanoparticles [60].

3.1.2 TEM analysis

Transmission electron microscopy studies have been conducted to analyze shape and size of the synthesized AgNps and support UV-visible spectroscopic analysis. This morphology can be more clearly seen in the magnified image in the inset of Figure 2. Observations show mainly three types of synthesized particles, spherical, triangular, hexagonal shape nanoparticles is also seen in Figure 2. Using the DLS technique, the size of the colloidal solutions of AgNps was determined to be between 12 nm and 60 nm. The reason for wide distribution of particle sizes of synthesized AgNps is due to biological complexity and natural variability of the compounds present in the plant extract. Z-average value was 113.1 nm. DLS size is always slightly larger than TEM [62].

3.1.3 X-Ray Diffraction Pattern (XRD)

X-ray diffraction measurements were performed to determine the crystallinity of AgNps. An X-ray diffractograph of AgNps synthesized is shown in the Figure 3. It is evident from the peaks, 27.92 (110), 32.27 (111), 38.17 (112), 46.31 (200), 57.62 (311) and 76.73 (311) planes of Bragg's reflections of metallic silver (Ag) with a lattice unit cell edge "a" = 4.0857, which is in good agreement with the FCC structure described by the Joint Committee of Powder Diffraction Standards (JCPDS). In accordance with the XRD analysis, the particles are AgNps. AgNps display strong and broad spectrum peaks, which indicate their crystalline nature and small

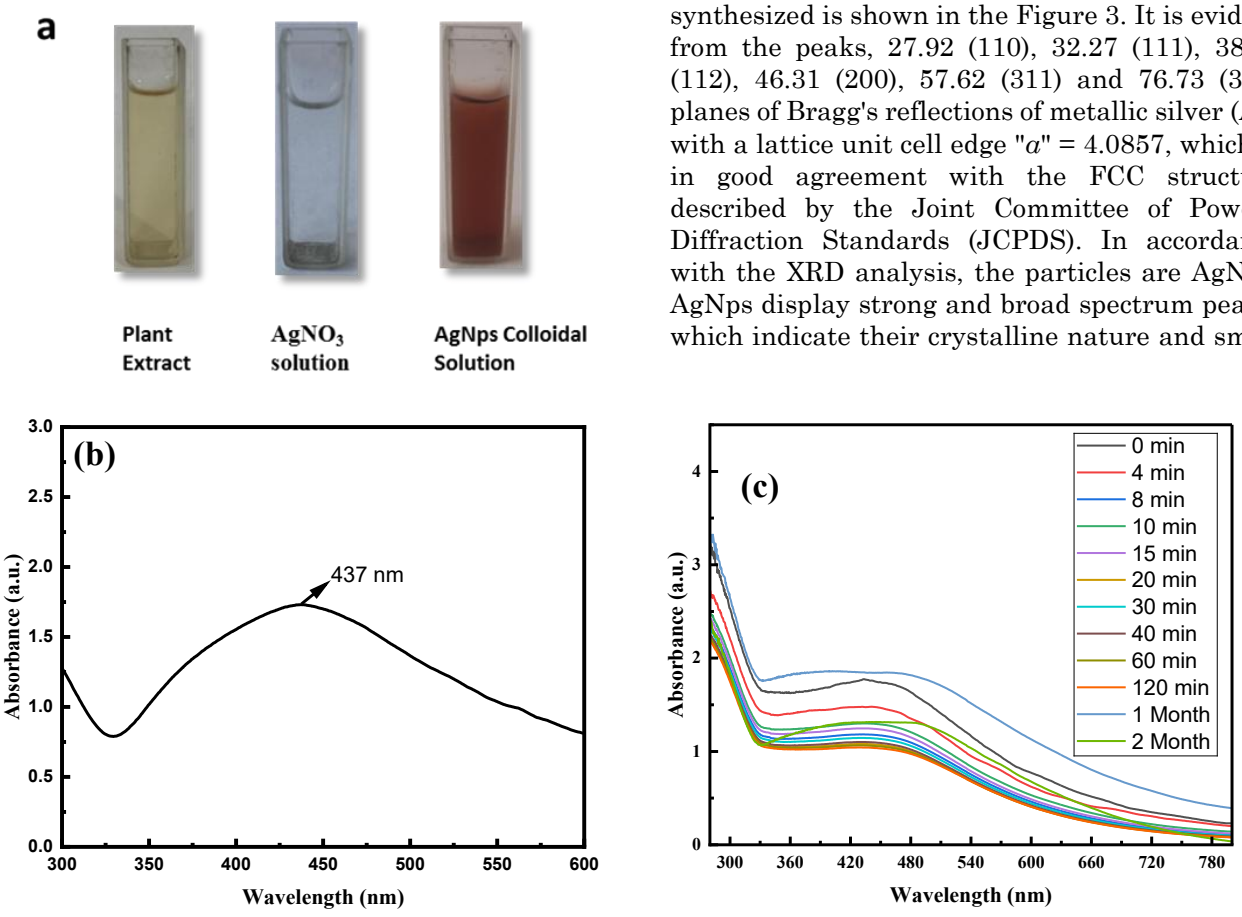

Figure 1. (a) Pictures of Plant extract, $AgNO_3$ solution, AgNps Colloidal Solution; (b) UV-Visible absorption spectra of synthesized AgNps stabilized in black cardamom; (c) at different time intervals from 0 to 2 month.

particle size also reported by Mishra *et al*. [50] (JCPDS-04-0783 & 084-0713). Based on the observed relationship between all planes in XRD peaks, all similar planes are the same 2θ value. Using the Debye Scherrer equation [63]:

$$D = 0.9\lambda/\beta \cos \theta \quad (3)$$

where D is the crystallite size, λ is the wavelength of X-ray used (1.5406 Å), β is the full width at half maximum (FWHM) and θ is the Bragg's angle. The average nanoparticle size is calculated to be 20.73 which is in well agreement with the DLS and TEM studies. Using the Bragg's equation, $n\lambda = 2d \sin \theta$ [64], d-spacing is calculated, and d-spacing is found to be 2.35 nm in this case.

3.1.4 Fourier Transform Infrared Spectroscopy (FTIR)

FTIR spectroscopy was used to investigate plant extract to determine their role in providing stability to the nanoparticles [60]. The chemical components present in the black cardamom extract can be identified by examining its FTIR spectra. 30 µL of black cardamom extract was used to record the FTIR spectra before and after the bioreduction of silver nanoparticles as shown in Figure 4. FTIR spectrum of black cardamom extract before and after the bioreduction reveals some peaks in the 4000 to 3200 cm^{-1}. A wide peak at 3259 cm^{-1} is attributed to O-H stretching vibrations of different types of phenolic compounds. The peak at 2925cm^{-1} is indicative of stretching vibration of aliphatic C-H bond. It is possible to assign the strong band at 1637 cm^{-1} to aromatic ring's C=C stretching vibrations. The phenolic group's C-O stretching vibrations are shown by the peak at 1031cm^{-1}. There are additional bands up to 1800 cm^{-1} in both the spectra, that is, in the spectra acquired prior to and following the reduction. The bands from 1770 to 500 cm^{-1} are nearly identical to those prior to reduction and after reduction but with slightly different intensities. Certain peaks, such as those of phenolic compounds and aromatic ring C=C stretching, varies slightly before and after the plant extract is reduced. The functional groups present in plant extract like Amino ($–NH_2$), carboxyl (–COOH), hydroxyl (–OH), and carbonyl (C=O) act as stabilizing and capping agents. Phenolic –OH, aldehydes, and acid equivalents in the extract donate electrons to reduce Ag^+ to Ag^0. The disappearance of C-O stretch peak at 1031 and C-H stretch at 2959 and shifts in the peak position after reduction shows the involvement of these functional groups in stabilization of synthesized AgNps.

3.1.5 Dynamic Light Scattering (DLS)

By studying the dynamic light scattering of synthesized AgNps, it was possible to determine their polydispersive indexes and average hydrodynamic diameters [65]. Using the DLS technique, the size of the colloidal solutions of AgNps was determined to be between 12 nm and 60 nm. Z-average value was 113.1 nm (Figure 5a). DLS size is always slightly larger than TEM [62]. It is the size of the AgNps metal core, the

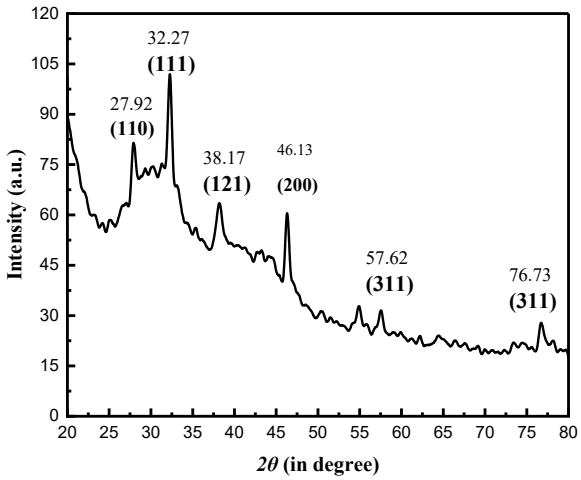

Figure 3. XRD pattern of synthesized AgNps

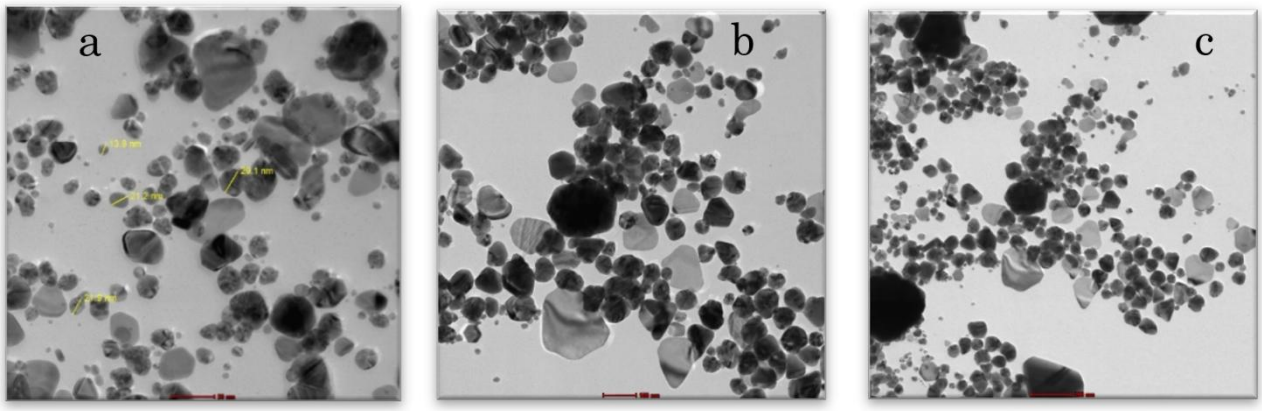

Figure 2. HR-TEM images of synthesized AgNps under different magnification (a) at 50 nm (b) at 100 nm (c) at 200 nm.

biomaterial embedded on their surface, and a liquid wall (solvent wall) that flows between the particles that determines the resulting size [66,67]. The PDI represents the size distribution within a sample [68]. Synthesized AgNps had a PDI value of 0.353, indicating that the nanoparticles are monodispersive. PDI values exceeding 0.7 indicate a broad particle size distribution that is unfavorable. As a general rule, the range of PDI values varies between 0.05 and 0.7, with values close to 0 indicating a monodispersive nature, and values near 1 indicating a polydispersive nature of nanoparticles. The zeta potential represents both the total charge that a particle receives in a given environment, as well as the surface charge of biogenic nanoparticles that is responsible for the development of propulsion forces between them. It is possible to determine the dispersion state of nanoparticles in a solution using the Zeta potential. There is a strong correlation between the zeta potential of the particles and the pH of the distribution, as well as the electrolyte. However, although the zeta potential is either higher than 30 mV or lower than 30 mV, the distribution remains stable [69]. The zeta potential value was −16.3 mV (Figure 5b). It is generally thought that particles with a negative charge typically have more stability because they are prevented from aggregating.

3.2 Applications

3.2.1 Catalytic activity of silver nanoparticles

3.2.1.1 Reduction of p-nitrophenol (4-NP)

The synthesized AgNps exhibited a high catalytic activity as revealed by the reduction of p-nitro phenol into p-amino phenol with degradation efficiency of 97.79%. The conversion reaction exhibits pseudo-first order kinetics with a rate constant of 0.422 minute^{-1}. We evaluated the catalytic activity of silver nanoparticles by reducing p-nitrophenol, a well-known pollutant and very stable compound that is difficult to degrade. To prevent photocatalytic reduction of p-nitrophenol, the entire process was carried out in dark conditions. As shown in Figure 6, p-nitro

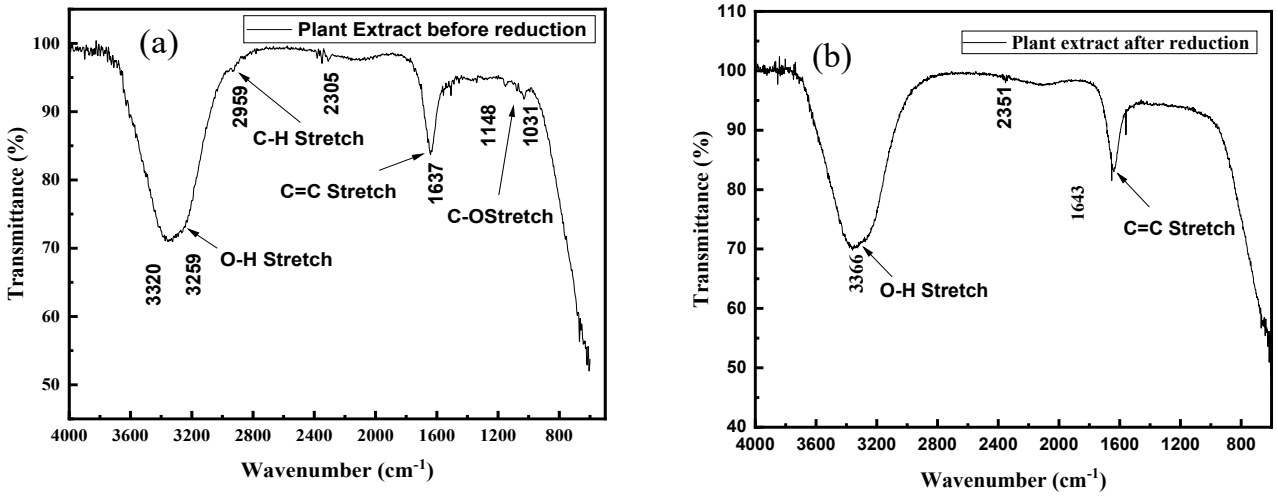

Figure 4. FT-IR spectra of plant extract (a) before reduction and (b) after reduction of plant extract.

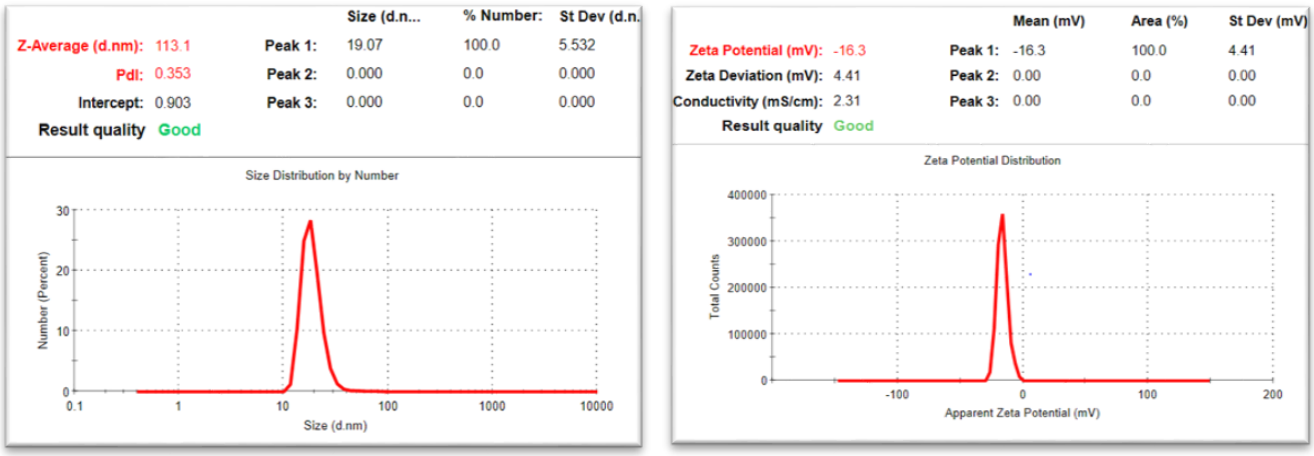

Figure 5. Showing the (a) size distribution and (b) Zeta potential of AgNps.

phenol is converted into p-amino phenol by p-nitro phenolate ions. Figure 6 (i) show the absorption maximum of p-nitrophenol at peak 317 nm and after adding $NaBH_4$ to p-nitrophenol, its color changes to yellow due to formation of sodium p-nitrophenolate and absorption maximum appears at 400nm. the interconversion of p-nitrophenolate into p-aminophenol took place after 55 min. However, as silver nanoparticles added, the catalytic reduction of sodium p-nitrophenolate happened very fast as shown in Figure 6a; the absorbance of peak at 400 nm decreases and it nearly becomes parallel to x-axis and there is simultaneous formation of p-nitro phenol appears by increase in absorbance of peak at 300 nm. So, we conclude that the reduction happened in just 10 minutes which is in agreement with previously reported studies as well [5,9]. Consequently, silver nanoparticles function as a catalyst and assist in the reduction of 4-NP by decreasing the reaction's activation energy. The absorbance of 4-NP is proportional to its initial concentration A_0 at time $t = 0$ and its concentration at time t is A_t. Based on the formula below, degradation efficiency between 4-NP and 4-AP was determined as follow:

$$Degrad.\ Efficiency\ (\%) = (A_o\text{-}A_t)/A_t \times 100\% \qquad (4)$$

Because the concentration of $NaBH_4$ was too high as compared to the concentration of 4-NP, the reduction of 4-NP to 4-AP by $NaBH_4$ in the presence of silver nanoparticles as catalyst results in a pseudo first order rate of reaction. It was therefore believed that the sodium borohydride concentration remained constant during the reaction. Figure 6 (ii) shows the UV-Vis spectra of the continuous reduction of 4-NP to 4-AP using AgNps at 10-min intervals. The degradation in absence of AgNps is in which is very high as compared to AgNps as shown in Figure 6b. The rate formula is expressed as:

$$K = \ln (A_0/A_t) / time \qquad (5)$$

The rate constant of the reaction for silver nanoparticles stabilized in black cardamom is found to be in Figure 6c, which displays a strong linear association between $\ln (A/A_o)$ and time.

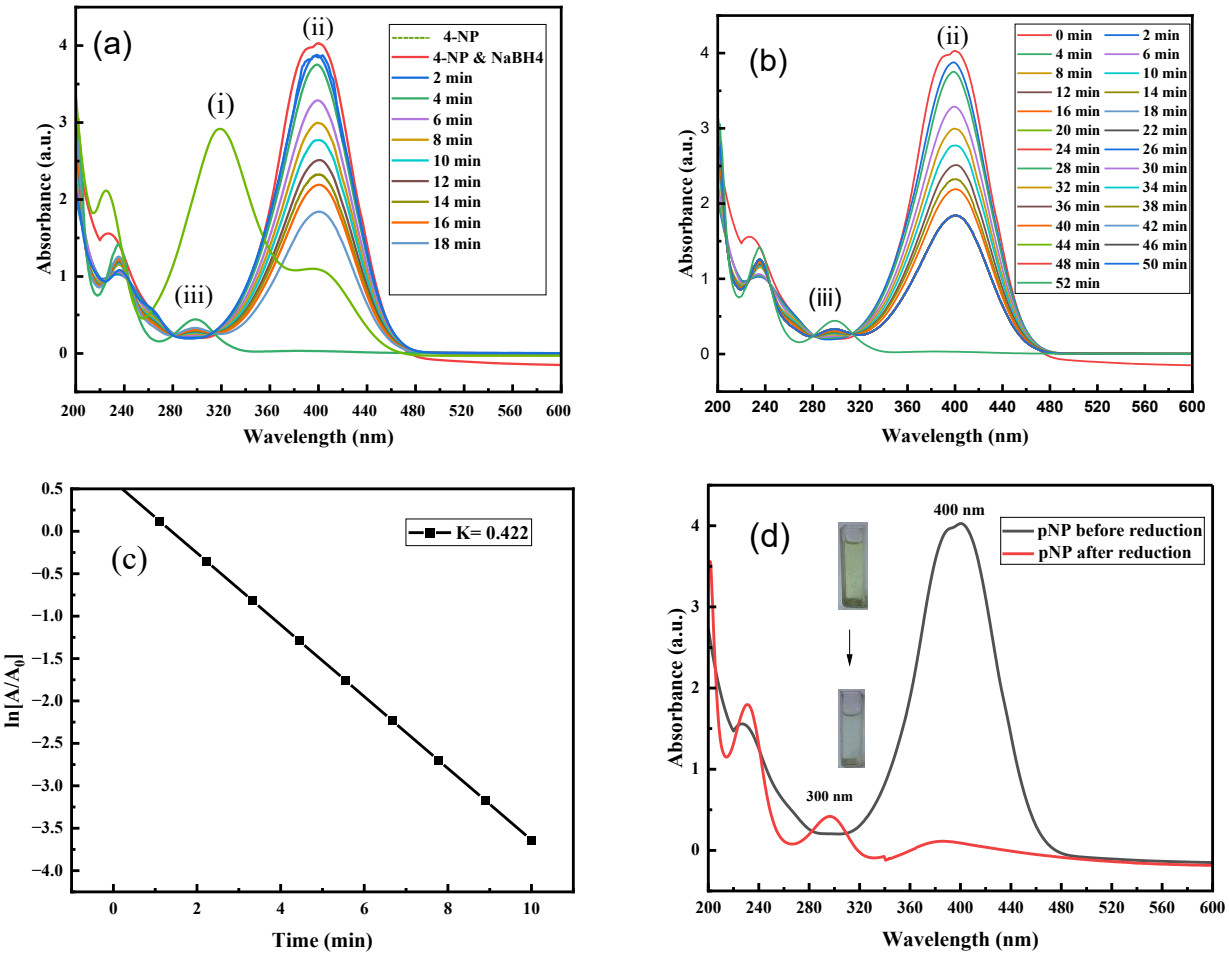

Figure 6. UV-visible spectra of (i) p-nitro phenol (1.9 mL, 0.2 mM) (ii) consecutive reduction of nitrophenolate ion with time interval of 2 min reacting with $NaBH_4$ (1 mL, 15 mM) (iii) p-amino phenol (a) in presence of Nano catalyst AgNps (10 µL,1.0 mg/mL); (b) in absence of AgNps ; (c) Plots of ln [A/A_o] against time for the conversion of p-nitrophenol into p-amino phenol using Silver nanoparticles; (d) reduction of p-nitro phenol into p-amino phenol.

3.2.1.2 Reduction/degradation of organic dyes (methylene blue)

Methylene blue, a thiazine dye used in aquatic life can detect trace levels of sulphide ions using Methylene Blue (MB). Aquaculture uses MB's cationic form as an antimicrobial and chemotherapeutic agent. In addition to its use in surgery, microbiology and diagnostics, MB has also been used in other fields [70]. Organic Dyes lead to do color contamination of various water bodies. So, act as toxic substance. Many aesthetic problems cause by textiles, dye and printing industries. Dye compounds used in such industries also have an adverse effect on aquatic life. Human health also gets disturbed by regular drinking of this toxic water. Textile industry produces MB; a heterocyclic dye absorbs at 664 nm showing n-π transition. In this degradation process, Silver nanoparticles act as heterogenous catalyst so increased the degradation rate of MB in the presence of a reducing agent $NaBH_4$. The MB dye did not show any color change when only $NaBH_4$ was added (Figure 7), but when Silver nanoparticles was added it get decolourize by forming leuco methylene blue which is measured by decrease in absorbance and complete

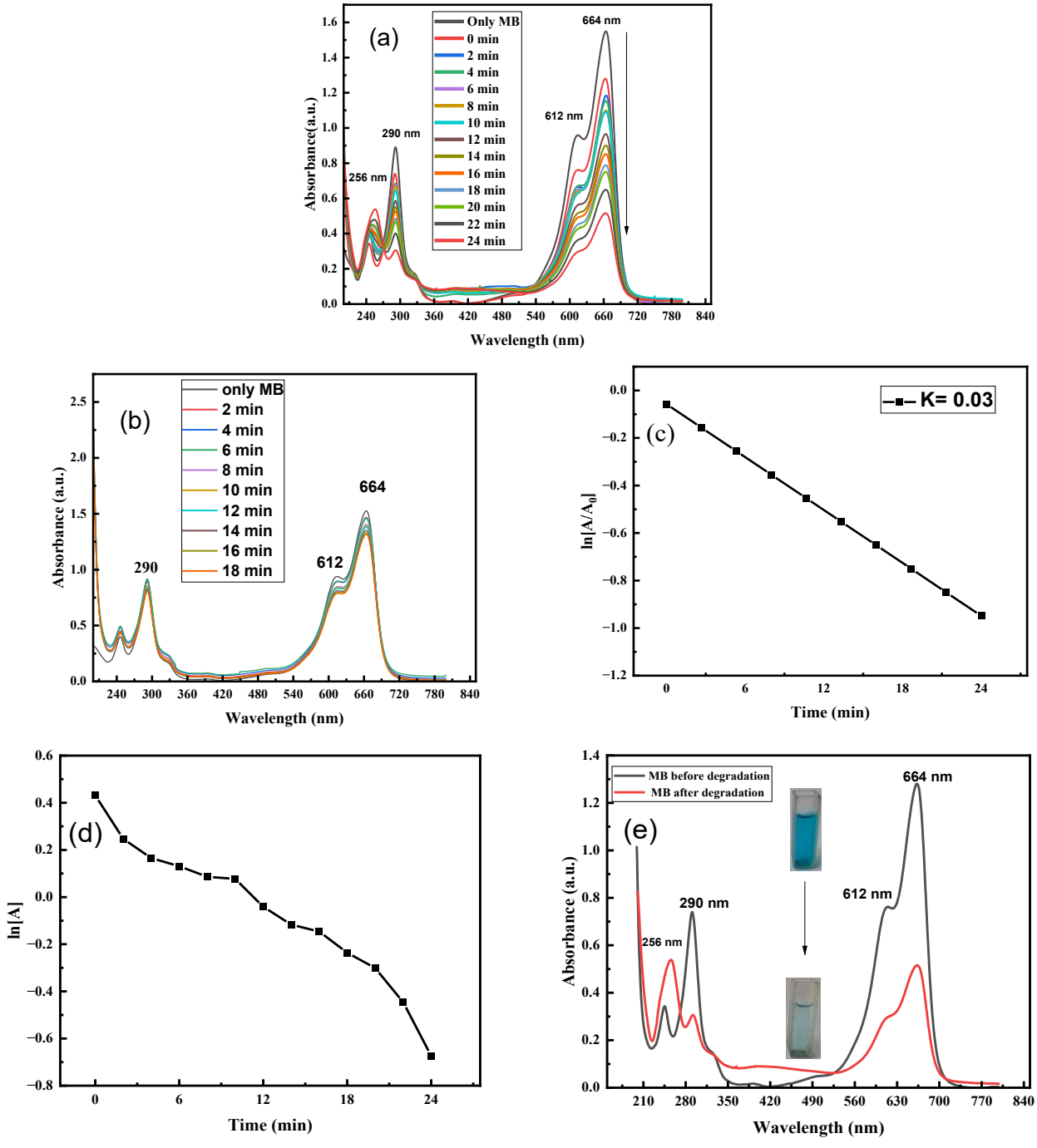

Figure 7. UV-visible spectra of successive degradation of methylene blue (2.5 mL, 10 mg/L): (a) in presence of nanocatalyst AgNps (20 µL, 1.0 mg/mL); (b) in absence of AgNps; (c) Plot of ln [A/A_0] against time; (d) Smooth plots of ln [A] against time; (e) Methylene blue before and after the degradation.

degradation takes place in 24 minutes which is represented in Figure 7a. Reaction increases many folds when AgNps act as catalyst. Rate constant calculated is 0.0376 min^{-1}.

For control, Reaction between MB and $NaBH_4$ also takes place but no significant decrease in absorbance takes place in absence of AgNps (Figure 7b).

The synthesized AgNps exhibited a high Catalytic activity for synthesized AgNps as recorded for the degradation of two water soluble dyes, MB and MO. Degradation efficiency 66.88% and 65.51% respectively. Kinetic study of the degradation reaction revealed the rates to be pseudo-first order with rate constants 0.0377 min^{-1} and 0.1016 min^{-1} for MB and MO respectively as shown in Figure 7c.

It has been observed that high reactivity and surface area of AgNps enhanced the rate of degradation of MB in the presence of $NaBH_4$ when AgNPs were added as heterogeneous catalysts. when $NaBH_4$ was added alone, MB dye did not have any visible change in absorbance as illustrated in Figure 7b. The blue color of the solution changed to colorless when AgNps were added, resulting in the compound, leuco methylene blue (LMB), which had a dip in absorbance between 665 and 670 nm. Figure 7e shows how the color of the methylene blue changes. Additionally, the reduction activity of AgNps alone for MB dye was also investigated, which revealed no differences in the dye's color or absorbance values, indicating that successful completion of this transformation required the use of a reducing agent. Due to their large surface area, MB and borohydride ions were able to adsorb on AgNps.

There were no visible changes seen after 40 minutes of $NaBH_4$ treatment. However, the dye degraded very quickly when AgNPs and $NaBH_4$ were present and the MB degradation was completed in 10 minutes. The rate formula is expressed as:

$$K = \ln (A_0/A_t) \ / \ time \qquad (6)$$

The rate constant of the reaction for silver nanoparticles stabilized in black cardamom is found to be 0.03 min^{-1} using Equation (6) and depicted in Figure 7c, which displays a strong linear association between ln (A_0/A_t) and time. Figure 7d shows that the original absorption peak at 664 nm progressively decreased with time, which confirms the degradation of methylene blue of the synthesized AgNps.

3.2.1.3 Degradation of organic dye Methyl Orange (MO)

MO is an organic azo dye used to add color to a variety of products in the paper, textile, and dye industries. But dye degradation is not an easy task. They must undergo several processes to convert into harmless, colorless elements. The best way to degrade MO is to react with $NaBH_4$ in the presence of AgNps. In mechanistic terms, $NaBH_4$ forms a layer on AgNps that encourages MO adsorption. Since AgNps is highly reactive and has a large surface area, dye molecules and reducing agents bind efficiently to its surface for a prolonged period of time, facilitating electron transfer from the borohydride anion to MO. As a result of the reaction, an intermediate is formed, followed by azo dye oxidation to colorless compounds. MO dye did not show any color change when only $NaBH_4$ was added, but when AgNps was added it get decolorize which is measured by decrease in absorbance and complete degradation takes place only in 10 minutes which is represented in Figure 8a.

Rate constant was calculated and it is found to be 0.10 min^{-1}. For control, reaction between MO and $NaBH_4$ also takes place but no significant decrease in absorbance takes place in 30 minutes in the absence of AgNPs. The rate calculated in both catalytic conversion of p-nitro phenol and dye degradation of MB and MO was found to be same as calculated using formula and from graph. The rate formula is expressed in Equation (6). The rate constant of the reaction for silver nanoparticles stabilized in black cardamom is found to be 0.10 min^{-1} using Equation (6) as shown in Figure 8c, which displays a strong linear association between ln (A_0 /A_t) and time. Figure 8 (d) represents the smooth plot of ln [A] vs time for the degradation of MO. The original absorption peak at 464 nm progressively decreased with time, which confirms the degradation of Methyl Orange of the synthesized AgNps.

Figure 9 and Table 1 show the schematic representation of catalytic activity: The synthesized AgNps act as catalyst by accepting electrons from BH_4 and donating them to p-nitro phenol, methyl orange, methylene blue act as an electron transfer mediator between AgNps and organic dyes by acting as a redox catalyst, which is often known as electron relay effect [1]. This is the mechanism where AgNps acting as a catalyst facilitate the transfer of electron between $NaBH_4$ and dye molecule. In this process, AgNps facilitate the transfer of electron between different chemical species, leading to their transformation. Methyl Orange loses electron (oxidation). Methyl orange breakdown into 4-(Dimethylamino) aniline and 4-aminobenzene sulphonic acid (colourless). Methlene blue into Leuco methylene blue (colourless). 4-Nitrophenol (yellow) into 4-amino phenol (colourless). So, AgNps act as catalyst which degrade organic dyes.

3.2.2 Antibacterial efficacy of AgNps

The anti-bacterial efficacy of prepared AgNps was determined against few gram-positive and gram- negative human pathogenic bacteria by measuring their size of ZoI as depicted in Figure 10 and Table 2. The results show that the biosynthesized nano-particles showed antibacterial activity. The sensitivity of bacteria with nano-particles (15 mg/mL) found to be more with *P. aeruginosa* than others as ZoI for *P. aeruginosa* (13 mm) > *E. coli* (12 mm) > *S. aureus* (10 mm) > *B. subtilis* (8 mm). The AgNPs exhibit inhibition zone formation though not at all the concentrations. The diameter of the ZOI is not comparable than positive control still the nano-particle is showing some antibacterial activity. ZOI of AgNps at various concentration with different bacteria as shown in Figure 10. The bar graph illustrates the zone of inhibition (in mm) of different bacteria at varying concentrations of AgNps (1,5,10,15 mg/mL) which is acting as a drug. So, this bar graph is showing that AgNps are

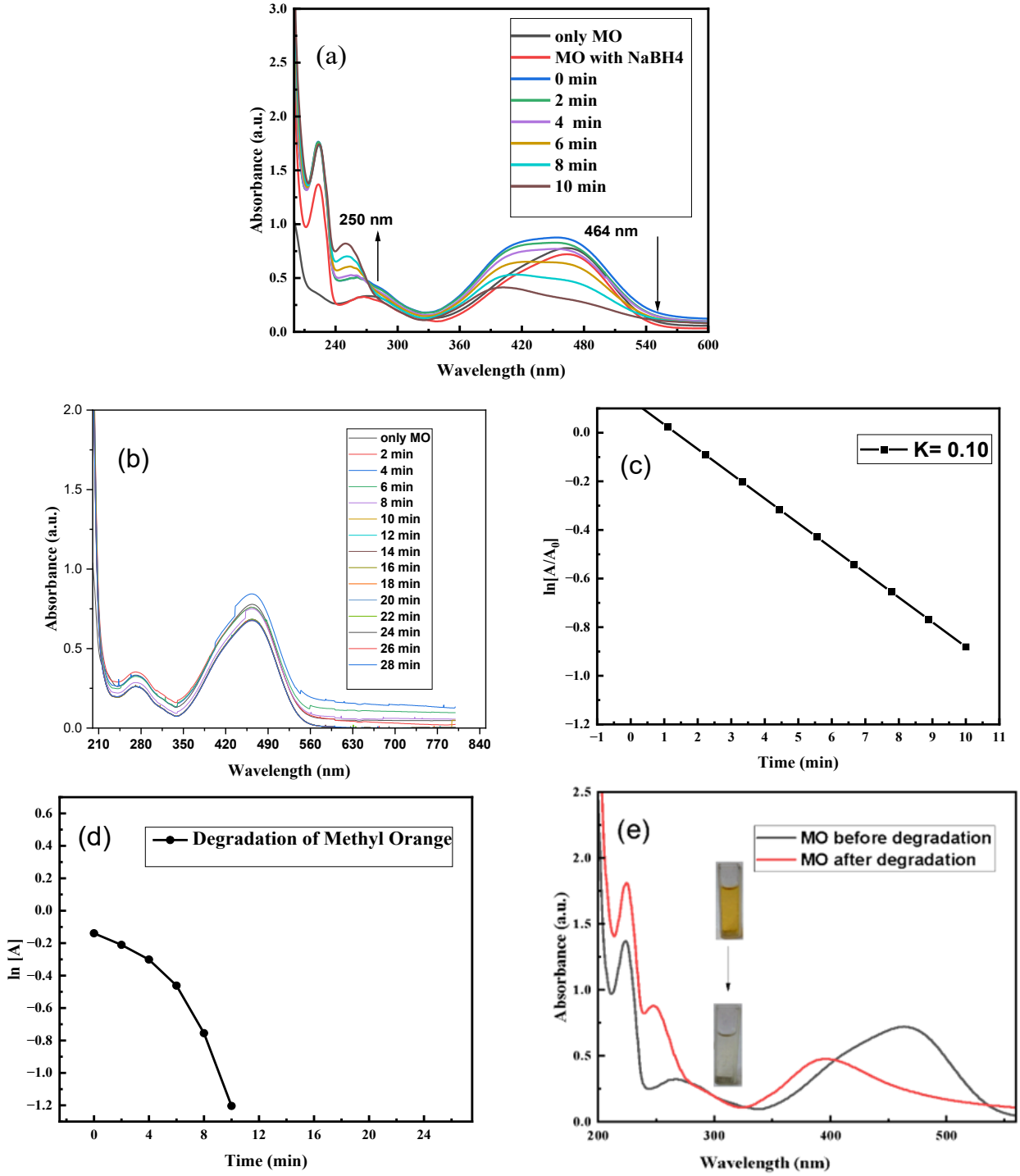

Figure 8. UV-visible spectra of Successive degradation of Methyl Orange (2.5 mL, 10 mg/L) in presence of $NaBH_4$ (100 µL, 0.2 M) (a) in presence of nanocatalyst AgNps (20 µL, 1.0 mg/mL); (b) in absence of AgNps; (c) Plot of ln [*A*/*A*o] against time; (d) Smooth plots of ln [*A*] against time; (e) Methylene Orange before and after the degradation.

acting as antibacterial agent. *E. Coli* shows moderate inhibition at all concentrations but slight increase at 15 mg/mL. Streptococcus exhibits the highest inhibition particularly at 10 and 15 mg/mL. Bacillus subtilis displays relatively low inhibition across all concentration. Pseudomonas shows inhibition maximum at 15 mg/mL.

3.2.3 Antioxidant activity: DPPH radical scavenging activity assay

DPPH is a free radical with a nitrogen center that can accept electrons and hydrogen radicals to form a stable diamagnetic molecule. Blank containing 2 mL methanol and 1 mL of 1,1-Diphenyl-2-picrylhydrazyl radical (DPPH) solution showed maximum absorbance at 517 nm. Biosynthesized AgNps demonstrated DPPH

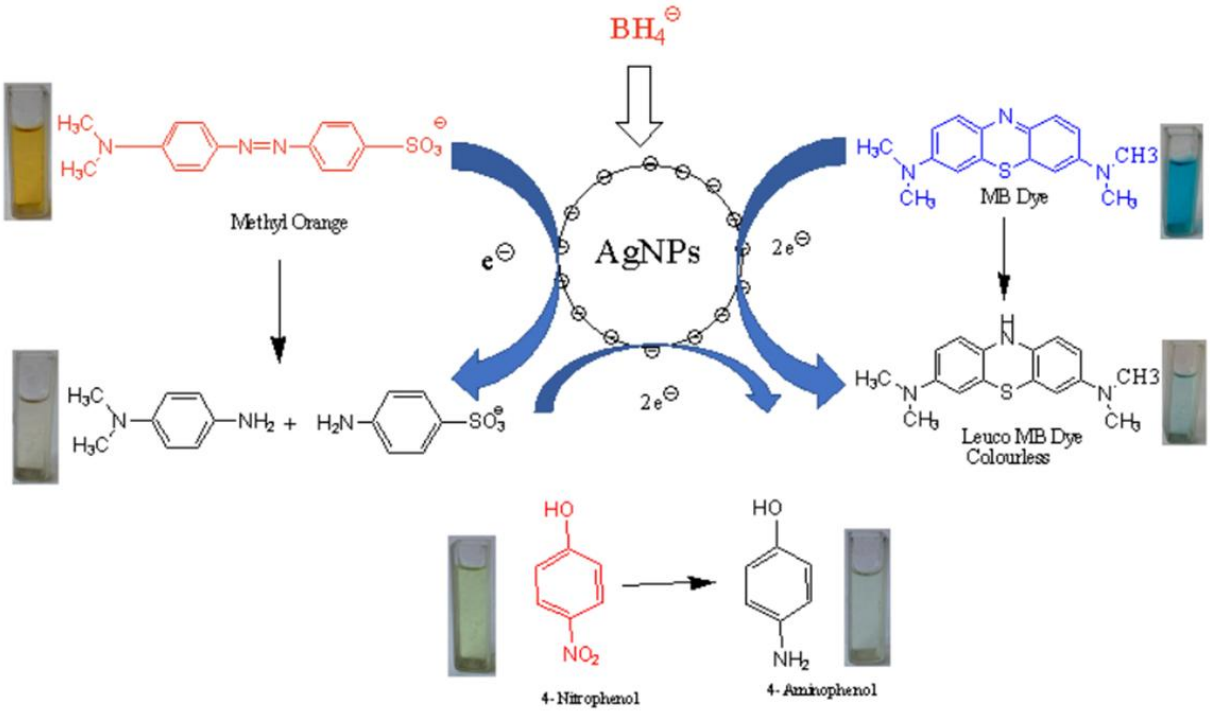

Figure 9. Schematic representation of catalytic activity of AgNps.

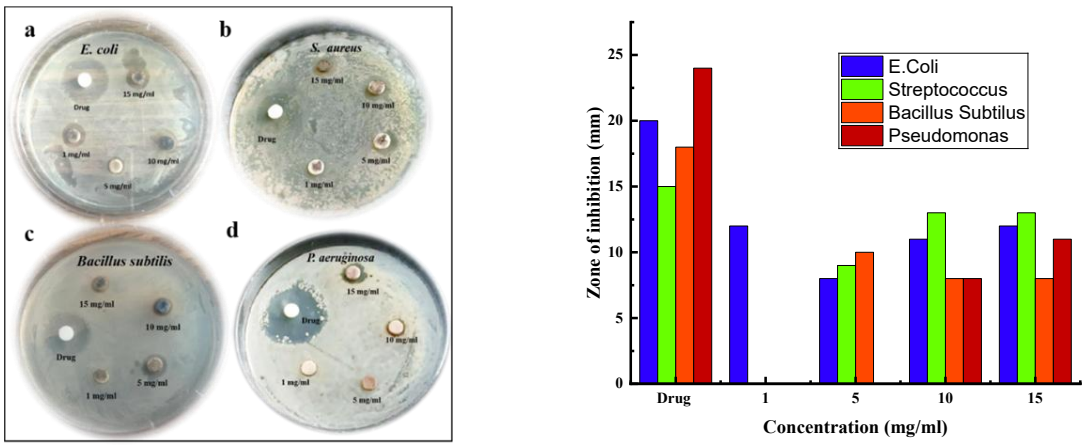

Figure 10. Antimicrobial activity of AgNps by disk diffusion method of (a) Escherichia coli; (b) Staphylococcus aureus; (c) Bacillus subtilis; (d) Pseudomonas aeruginosa (left) Graph between Zone of inhibition and different concentration of drug and synthesized AgNps (right).

Table 1. Catalytic activity of AgNps in the degradation of MO and MB.

Dyes	AgNps concentration	Reaction time (minute)	*K* (min^{-1})	Correlation Coefficient (R^2)
Methylene Blue	1 mg/mL	12	0.0377	0.95015
Methyl Orange	1mg/mL	8	0.10168	0.86053

radical scavenging activity. According to UV-Visible measurements, the violet color of AgNps and ascorbic acid indicates the antioxidant activity of these compounds. AgNps and ascorbic acid percentage scavenging values versus concentration are shown in Figure 11. Both AgNps and ascorbic acid demonstrated an increase in scavenging ability with increasing concentrations, as can be seen in the graph. While ascorbic acid was capable of neutralizing DPPH radical to 98%, AgNps were able to scavenge 75% at 1500 µg/mL. As a result, The observed antioxidant of AgNPs can be attributed to the presence of hydroxyl and carboxyl groups on their surface, which are believed to act as reducing agents, and to Ag(0), given that Ag(0) is able to donate one electron to become Ag^+.

4. Conclusions

In this study, stable AgNps were prepared via green synthesis using seeds of black cardamom. The synthesis of AgNps was carried out in aqueous medium without using any toxic chemicals. The synthesized AgNps were found to be stable over a period of two months as revealed by UV-vis spectra. Through this method, well dispersed and crystalline AgNps were obtained and characterized by UV-Visible, FTIR, XRD and TEM techniques. The synthesized AgNps proved to act as catalysts and reduced 4 NP to 4 AP and it is determined that the reaction is pseudo-first order by kinetic studies. The synthesized AgNps reduced the MB and MO organic dyes. This green method of preparation of AgNps can be extended for large scale production which can be used for various biomedical application and environmental remediation etc.

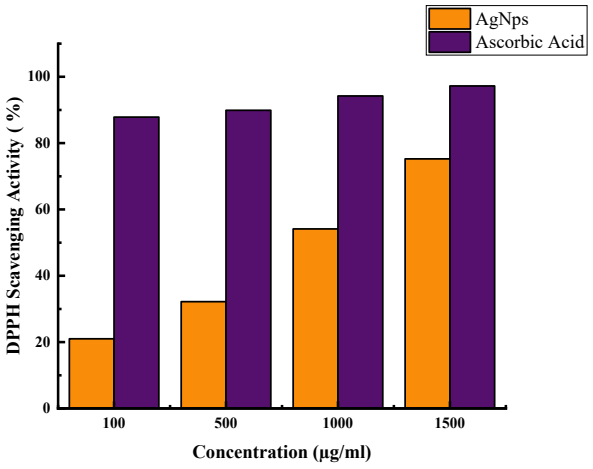

Figure 11. Bar graph of antioxidant activity of synthesized AgNps by DPPH.

Acknowledgments

We acknowledge University Science Instrumentation Centre (USIC), Delhi University, New Delhi for XRD measurements and Sophisticated Analytical Instrumentation Facility (SAIF), AIIMS, New Delhi for TEM and DLS measurements.

CRedit Author Statement

Author Contributions: S. Baghel: Experiments, Data Analysis, Writing-Original Draft; M. Khurana: Conceptualization, Resources, Supervision, Review and Editing; P. Gupta: Writing and Editing. All authors have read and agreed to the published version of the manuscript.

References

[1] Dhiman, J., Kundu, V., Kumar, S., Kumar, R., Chakarvarti, S.K. (2014). Eco-friendly Synthesis and Characterization of Silver Nanoparticles and Evaluation of Their Antibacterial Activity. *American Journal of Materials Science and Technology*, 3(1), 13–21. DOI: 10.7726/ajmst.2014.1002.

[2] Vasireddy, R., Paul, R., Mitra, A.K. (2012). Green synthesis of silver nanoparticles and the study of optical properties. *Nanomaterials and Nanotechnology*, 2(1), 1–6. DOI: 10.5772/52329.

[3] Ghosh, T., Chattopadhyay, A., Mandal, A.C., Pramanik, S., Kuiri, P.K. (2020). Optical, structural, and antibacterial properties of biosynthesized Ag nanoparticles at room temperature using Azadirachta indica leaf extract. *Chinese Journal of Physics*, 68, 835–848. DOI: 10.1016/j.cjph.2020.10.025.

[4] Khan, A.N., Ali Aldowairy, N.N., Saad Alorfi, H.S., Aslam, M., Bawazir, W.A.B., Hameed, A., Soomro, M.T. (2022). Excellent Antimicrobial, Antioxidant, and Catalytic Activities of Medicinal Plant Aqueous Leaf Extract Derived Silver Nanoparticles. *Processes*, 10(10), 1–24. DOI: 10.3390/pr10101949.

Table 2. Catalytic activity of AgNps in the degradation of MO and MB.

Test organism/ Zone of Inhibition (mm)	Drug (Streptomycin)	1 mg/mL	5 mg/mL	10 mg/mL	15 mg/mL
E. coli	20	12	8	11	12
Streptococcus Aureus	15	-	9	13	13
Bacillus Subtilus	18	-	10	8	8
Pseuduomonas	24	-	-	8	11

[5] Mahiuddin, M., Saha, P., Ochiai, B. (2020). Green synthesis and catalytic activity of silver nanoparticles based on piper chaba stem extracts. *Nanomaterials*, 10(9), 1–15. DOI: 10.3390/nano10091777.

[6] Borhamdin, S., Shamsuddin, M., Alizadeh, A. (2016). Biostabilised icosahedral gold nanoparticles: synthesis, cyclic voltammetric studies and catalytic activity towards 4-nitrophenol reduction. *Journal of Experimental Nanoscience*, 11(7), 518–530. DOI: 10.1080/17458080.2015.1090021.

[7] Seo, Y.S., Ahn, E.Y., Park, J., Kim, T.Y., Hong, J.E., Kim, K., Park, Y., Park, Y. (2017). Catalytic reduction of 4-nitrophenol with gold nanoparticles synthesized by caffeic acid. *Nanoscale Research Letters*, 12(1), 1–11. DOI: 10.1186/s11671-016-1776-z.

[8] Thomas, O.E., Alabi, O.S., Osharode, P.E. (2023). Characterization, antimicrobial and catalytic activities of silver nanoparticles biosynthesized using aqueous extract of Euphorbia graminea. *Acta Pharmaceutica Sciencia*, 61(2), 165–182. DOI: 10.23893/1307-2080.APS6112.

[9] Venkatesham, M., Ayodhya, D., Madhusudhan, A., Santoshi Kumari, A., Veerabhadram, G., Girija Mangatayaru, K. (2014). A Novel Green Synthesis of Silver Nanoparticles Using Gum Karaya: Characterization, Antimicrobial and Catalytic Activity Studies. *Journal of Cluster Science*, 25(2), 409–422. DOI: 10.1007/s10876-013-0620-1.

[10] Wu, S., Yan, S., Qi, W., Huang, R., Cui, J., Su, R., He, Z. (2015). Green synthesis of gold nanoparticles using aspartame and their catalytic activity for p-nitrophenol reduction. *Nanoscale Research Letters*, 10(1), 0–6. DOI: 10.1186/s11671-015-0910-7.

[11] Roy, A., Mohanta, B. (2019). Microwave-assisted green synthesis of Gold nanoparticles and its catalytic activity. *Autumn 2019 J Nano Dimens*, 10(4), 359–367.

[12] Ganash, A.A. (2019). Electrochemical properties and mechanistic study of the green synthesis of silver nanoparticles using Bardaqush extract solution. *Materials Research Express*, 6(6), 065024. DOI: 10.1088/2053-1591/ab0d40.

[13] Ismail, M., Xiangke, W., Khan, A.A., Khan, Q. (2023). Amomum subalatum leaf extract derived silver nanoparticles for eco-friendly spectrophotometric detection of Hg(II) ions in water. *Chemical Physics Impact*, 6(December 2022), 1–6. DOI: 10.1016/j.chphi.2022.100148.

[14] Keerthana, B., Geetha, R. V, Rajeshkumar, S. (2021). Evaluation of Antidiabetic and Cytotoxic Effect of Boerhavia Diffusa Mediated Selenium Nanoparticles. *Nat. Volatiles & Essent Oils*, 8(6), 5891–5900.

[15] Philip, D. (2010). Green synthesis of gold and silver nanoparticles using Hibiscus rosa sinensis. *Physica E: Low-Dimensional Systems and Nanostructures*, 42(5), 1417–1424. DOI: 10.1016/j.physe.2009.11.081.

[16] Rajalekshmi, Lohithan, R., Raj, R., Prakash, P., Santosh, A., Theertha, V., Chandran, S. (2020). Green synthesis of silver nanoparticles from Justicia adhatodaplant extract with its diverse properties. *Journal of Physics: Conference Series*, 1706(1), 1–4. DOI: 10.1088/1742-6596/1706/1/012012.

[17] Ahmad, N., Sharma, S. (2012). Green Synthesis of Silver Nanoparticles Using Extracts of Ananas comosus. *Green and Sustainable Chemistry*, 2(November), 141–147. DOI: 10.4236/gsc.2012.24020.

[18] Maity, G.N., Maity, P., Choudhuri, I. (2020). Green synthesis, characterization, antimicrobial and cytotoxic effect of silver nanoparticles using arabinoxylan isolated from Kalmegh. *International Journal of Biological Macromolecules*, 1–22. DOI: 10.1016/j.ijbiomac.2020.06.215.

[19] Rao, Y.S., Kotakadi, V.S., Prasad, T.N.V.K. V, Reddy, A. V, Gopal, D.V.R.S. (2013). Green synthesis and spectral characterization of silver nanoparticles from Lakshmi tulasi (Ocimum sanctum) leaf extract. *Spectrochimica Acta Part A : Molecular and Biomolecular Spectroscopy*, 103, 156–159. DOI: 10.1016/j.saa.2012.11.028.

[20] State, K. (2018). Biosynthesis of silver nanoparticles using azadirachta indica leaf extract and assessment of its antibacterial activity on some pathogenic enteric bacteria. *International Journal of Novel Research in Life Sciences*, 5(2), 2005–2011.

[21] Saxena, A., Tripathi, R.M., Singh, R.P. (2010). Synthesis of silver nanoparticles using onion (Allium cepa) extract and their antibacterial activity. *Digest Journal of Nanomaterials and Biostructures*, 5(April), 427–432.

[22] Amina, M., Musayeib, N.M. Al, Alarfaj, N.A., El-tohamy, M.F. (2020). Antibacterial and Immunomodulatory Potentials of Biosynthesized Ag , Au , Ag-Au Bimetallic Alloy Nanoparticles Using the Asparagus racemosus Root Extract. *nanomaterials*, 10(10), 2453. DOI: 10.3390/nano10122453.

[23] Sarkar, M., Denrah, S., Patra, M., Basu, T. (2020). Studies on the Antibacterial and Catalytic Activities of Silver Nanoparticles Synthesized from Cyperus rotundus L . *Journal of Cluster Science*, 9, 1–14. DOI: 10.1007/s10876-020-01785-9.

[24] Ahmad, N., Sharma, S., Shamsi, A., Narayan, A. (2014). Green Synthesis of Silver Nanoparticles by Exploiting Ayurvedic Plant Shalaparni. *Journal of Bionanoscience*, 8(1), 45–50. DOI: 10.1166/jbns.2014.1200.

[25] Kushwah, M., Bhadauria, S., Singh, K.P., Gaur, M.S. (2019). Antibacterial and Antioxidant Activity of Biosynthesized Silver Nanoparticles Produced by Aegle marmelos Fruit Peel Extract. *Analytical Chemistry Letters*, 7928, 329–344. DOI: 10.1080/22297928.2019.1626279.

[26] Sharada, S.O.V. (2015). Green Synthesis and Characterization of Silver Nanoparticles and Evaluation of their Antibacterial Activity using Elettaria Cardamom Seeds. *Journal of Nanomedicine & Nanotechnology*, 06(02), 2–5. DOI: 10.4172/2157-7439.1000266.

[27] Tian, Y., Luo, J., Wang, H., Zaki, H.E.M., Yu, S., Wang, X., Ahmed, T., Shahid, M.S., Yan, C., Chen, J., Li, B. (2022). Bioinspired Green Synthesis of Silver Nanoparticles Using Three Plant Extracts and Their Antibacterial Activity against Rice Bacterial Leaf Blight Pathogen Xanthomonas oryzae pv. oryzae. *Plants*, 11(21), 1–15. DOI: 10.3390/plants11212892.

[28] Ajaykumar, A.P., Mathew, A., Chandni, A.P., Varma, S.R., Jayaraj, K.N., Sabira, O., Rasheed, V.A., Binitha, V.S., Swaminathan, T.R., Basheer, V.S., Giri, S., Chatterjee, S. (2023). Green Synthesis of Silver Nanoparticles Using the Leaf Extract of the Medicinal Plant, Uvaria narum and Its Antibacterial, Antiangiogenic, Anticancer and Catalytic Properties. *Antibiotics*, 12(3), 1–16. DOI: 10.3390/antibiotics12030564.

[29] Rafi, A., Asif, M., Alam, T., Iqbal, Z., Tahir, Z., Elahi, F. (2020). Silver Nano Particles (AgNP) Synthesis Using Apple Extract. *Bulletin of Environment, Pharmacology and Life Sciences*, 9(10), 103–106.

[30] Pattanayak, M., Nayak, P.L. (2013). Green Synthesis of Gold Nanoparticles Using Elettaria cardamomum (ELAICHI) Aqueous Extract. *World Journal of Nano Science & Technology*, 2(1), 1–5. DOI: 10.5829/idosi.wjnst.2013.2.1.21131.

[31] Noah, N. (2019). Chapter 6: Green synthesis; Characterization and application of silver and gold nanoparticles. In *Green Synthesis, Characterization and Applications of Nanoparticles*, pp. 111–135. DOI: 10.1016/B978-0-08-102579-6.00006-X.

[32] Rastogi, L., Arunachalam, J. (2013). Green synthesis route for the size controlled synthesis of biocompatible gold nanoparticles using aqueous extract of garlic (Allium sativum). *Advanced Materials Letters*, 4(7), 548–555. DOI: 10.5185/amlett.2012.11456.

[33] Logan, T., Ly, M. (2013). Gold Nanoparticle Interaction with Cell Membranes. *Worcester Polytechnic Institute*, 1-102.

[34] Rao, B.L., Gouda, G.P., Shivananda, C.S. (2020). Green synthesis of silver nanoparticles using Hibiscus Rosa Sinensis flower extract. *3rd International Conference on Condensed Matter and Applied Physics (Icc-2019)*, 2220(May), 020103. DOI: 10.1063/5.0002996.

[35] Alex, K.V., Pavai, P.T., Rugmini, R., Prasad, M.S., Kamakshi, K., Sekhar, K.C. (2020). Green Synthesized Ag Nanoparticles for Bio-Sensing and Photocatalytic Applications. *ACS Omega*, 5, 13123–13129. DOI: 10.1021/acsomega.0c01136.

[36] Possomato-Vieira, José S. and Khalil, R.A.K., Modeling, O. 2. 0. E.S.E. and S. (2017). Hyperthermia Using Nanoparticles – Promises and Pitfalls. *Physiology & behavior*, 176(12), 139–148. DOI: 10.3109/02656736.2015.1120889.

[37] Zhang, D., Ma, X.L., Gu, Y., Huang, H., Zhang, G.W. (2020). Green Synthesis of Metallic Nanoparticles and Their Potential Applications to Treat Cancer. *Frontiers in Chemistry*, 8, 1–18. DOI: 10.3389/fchem.2020.00799.

[38] Borah, D., Das, N., Sarmah, P., Ghosh, K., Chandel, M., Rout, J., Pandey, P., Ghosh, N.N., Bhattacharjee, C.R. (2023). A facile green synthesis route to silver nanoparticles using cyanobacterium Nostoc carneum and its photocatalytic, antibacterial and anticoagulative activity. *Materials Today Communications*, 34, 105110. DOI: 10.1016/j.mtcomm.2022.105110.

[39] Dhir, S., Dutt, R., Singh, R.P., Chauhan, M., Virmani, T., Kumar, G., Alhalmi, A., Aleissa, M.S., Rudayni, H.A., Al-Zahrani, M. (2023). Amomum subulatum Fruit Extract Mediated Green Synthesis of Silver and Copper Oxide Nanoparticles: Synthesis, Characterization, Antibacterial and Anticancer Activities. *Processes*, 11(9), 2698. DOI: 10.3390/pr11092698.

[40] Ihsan, M., Niaz, A., Rahim, A., Zaman, M.I., Arain, M.B., Sirajuddin, Sharif, T., Najeeb, M. (2015). Biologically synthesized silver nanoparticle-based colorimetric sensor for the selective detection of Zn^{2+}. *RSC Advances*, 5(111), 91158–91165. DOI: 10.1039/c5ra17055a.

[41] Shan, B., Cai, Y.Z., Sun, M., Corke, H. (2005). Antioxidant capacity of 26 spice extracts and characterization of their phenolic constituents. *Journal of Agricultural and Food Chemistry*, 53(20), 7749–7759. DOI: 10.1021/jf051513y.

[42] Khuat, Q.V., Kalashnikova, E.A., Nguyen, H.T., Slovareva, O.Y., Kirakosyan, R.N. (2022). Antifungal activity of Black cardamom (Amomum tsao-ko Crevost et Lemairé) plant extracts against Fusarium oxysporum Schlechtend and their prospect of developing fungicide for sustainable agricultural production. *IOP Conference Series: Earth and Environmental Science*, 1112 (1). DOI: 10.1088/1755-1315/1112/1/012103.

[43] Preetha, D., Arun, R., Kumari, P., Aarti, C. (2013). Synthesis and characterization of silver nanoparticles using cannonball leaves and their cytotoxic activity against Mcf-7 cell line. *Journal of Nanotechnology*, 2013, 1–5. DOI: 10.1155/2013/598328.

[44] Vidyasagar, N., Patel, R.R., Singh, S.K., Singh, M. (2023). Green synthesis of silver nanoparticles: methods, biological applications, delivery and toxicity. *Materials Advances*, 4(8), 1831–1849. DOI: 10.1039/d2ma01105k.

[45] Sharifi-Rad, M., Pohl, P., Epifano, F., Álvarez-Suarez, J.M. (2020). Green synthesis of silver nanoparticles using astragalus tribuloides delile. Root extract: Characterization, antioxidant, antibacterial, and anti-inflammatory activities. *Nanomaterials*, 10(12), 1–17. DOI: 10.3390/nano10122383.

[46] Alduraihem, N.S., Bhat, R.S., Al-Zahrani, S.A., Elnagar, D.M., Alobaid, H.M., Daghestani, M.H. (2023). Anticancer and Antimicrobial Activity of Silver Nanoparticles Synthesized from Pods of Acacia nilotica. *Processes*, 11(2), 1–16. DOI: 10.3390/pr11020301.

[47] Aftab, R. A., Zaidi, S., Danish, M., Danish, M., Ansari, K. B., Rao, R. A. K., & Qyyum, M.A. (2023). Herbal medicinal waste black cardamom (Amomum subulatum) as a novel adsorbent for removing Cd(II) from water. *International Journal of Environmental Science and Technology*, 1–20. DOI: 10.1007/s13762-023-04996-5.

[48] Ahmad Aftab, R., Zaidi, S., Aslam Parwaz Khan, A., Arish Usman, M., Khan, A.Y., Tariq Saeed Chani, M., Asiri, A.M. (2023). Removal of congo red from water by adsorption onto activated carbon derived from waste black cardamom peels and machine learning modeling. *Alexandria Engineering Journal*, 71, 355–369. DOI: 10.1016/j.aej.2023.03.055.

[49] Singh, A.K., Tripathi, M., Srivastava, O.N., Verma, R.K. (2017). Silver Nanoparticles/Gelatin Composite: A New Class of Antibacterial Material. *ChemistrySelect*, 2(24), 7233–7238. DOI: 10.1002/slct.201701245.

[50] Mishra, A.K., Tiwari, K.N., Saini, R., Kumar, P., Mishra, S.K., Yadav, V.B., Nath, G. (2020). Green Synthesis of Silver Nanoparticles from Leaf Extract of Nyctanthes arbor-tristis L. and Assessment of Its Antioxidant, Antimicrobial Response. *Journal of Inorganic and Organometallic Polymers and Materials*, 30(6), 2266–2278. DOI: 10.1007/s10904-019-01392-w.

[51] Holzwarth, U., Gibson, N. (2011). The Scherrer equation versus the "Debye-Scherrer equation." *Nature Nanotechnology*, 6(9), 534. DOI: 10.1038/nnano.2011.145.

[52] Wang, J., Li, Y., Lu, Q., Hu, Q., Liu, P., Yang, Y., Li, G., Xie, H., Tang, H. (2021). Drying temperature affects essential oil yield and composition of black cardamom (Amomum tsao-ko). *Industrial Crops and Products*, 168. DOI: 10.1016/j.indcrop.2021.113580.

[53] Singh, A.K., Srivastava, O.N. (2015). One-Step Green Synthesis of Gold Nanoparticles Using Black Cardamom and Effect of pH on Its Synthesis. *Nanoscale Research Letters*, 10(1), 1–12. DOI: 10.1186/s11671-015-1055-4.

[54] Majumdar, R., Bag, B.G., Maity, N. (2013). Acacia nilotica (Babool) leaf extract mediated size-controlled rapid synthesis of gold nanoparticles and study of its catalytic activity. *International Nano Letters*, 3(53), 1–6. URL: http://www.inl-journal.com/content/3/1/53.

[55] Singh, I., Gupta, S., Gautam, H.K., Dhawan, G., Kumar, P. (2021). Antimicrobial, radical scavenging, and dye degradation potential of nontoxic biogenic silver nanoparticles using Cassia fistula pods. *Chemical Papers*, 75(3), 979–991. DOI: 10.1007/s11696-020-01355-3.

[56] Rauf, M.A., Meetani, M.A., Khaleel, A., Ahmed, A. (2010). Photocatalytic degradation of Methylene Blue using a mixed catalyst and product analysis by LC/MS. *Chemical Engineering Journal*, 157(2), 373–378. DOI: 10.1016/j.cej.2009.11.017.

[57] Flores, N.M., Pal, U., Galeazzi, R., Sandoval, A. (2014). Effects of morphology, surface area, and defect content on the photocatalytic dye degradation performance of ZnO nanostructures. *RSC Adv.*, 4(77), 41099–41110. DOI: 10.1039/C4RA04522J.

[58] Soshnikova, V., Kim, Y.J., Singh, P., Huo, Y., Markus, J., Ahn, S., Castro-Aceituno, V., Kang, J., Chokkalingam, M., Mathiyalagan, R., Yang, D.C. (2018). Cardamom fruits as a green resource for facile synthesis of gold and silver nanoparticles and their biological applications. *Artificial Cells, Nanomedicine and Biotechnology*, 46(1), 108–117. DOI: 10.1080/21691401.2017.1296849.

[59] Lo, K.M., Cheung, P.C.K. (2005). Antioxidant activity of extracts from the fruiting bodies of Agrocybe aegerita var. alba. *Food Chemistry*, 89 (4), 533–539. DOI: 10.1016/j.foodchem.2004.03.006.

[60] Joseph, S., Mathew, B. (2015). Microwave-assisted green synthesis of silver nanoparticles and the study on catalytic activity in the degradation of dyes. *Journal of Molecular Liquids*, 204, 184–191. DOI: 10.1016/j.molliq.2015.01.027.

[61] Moores, A., Goettmann, F. (2006). The plasmon band in noble metal nanoparticles: an introduction to theory and applications. *New J. Chem.*, 30 (8), 1121–1132. DOI: 10.1039/B604038C.

[62] Boruah, J.S., Devi, C., Hazarika, U., Bhaskar Reddy, P.V., Chowdhury, D., Barthakur, M., Kalita, P. (2021). Green synthesis of gold nanoparticles using an antiepileptic plant extract: in vitro biological and photo-catalytic activities. *RSC Advances*, 11(45), 28029–28041. DOI: 10.1039/D1RA02669K.

[63] Bykkam, S., Ahmadipour, M., Narisngam, S., Kalagadda, V.R., Chidurala, S.C. (2015). RETRACTED: Extensive Studies on X-Ray Diffraction of Green Synthesized Silver Nanoparticles. *Advances in Nanoparticles*, 04(01), 1–10. DOI: 10.4236/anp.2015.41001.

[64] Theivasanthi, T., Alagar, M. (2012). Electrolytic Synthesis and Characterizations of Silver Nanopowder. *Nano Biomedicine and Engineering*, 4(2), 1–12. DOI: 10.48550/arXiv.1111.0260.

[66] Jalab, J., Abdelwahed, W., Kitaz, A., Al-Kayali, R. (2021). Green synthesis of silver nanoparticles using aqueous extract of Acacia cyanophylla and its antibacterial activity. *Heliyon*, 7(9), e08033. DOI: 10.1016/j.heliyon.2021.e08033.

[67] Rezazadeh, N.H., Buazar, F., Matroodi, S. (2020). Synergistic effects of combinatorial chitosan and polyphenol biomolecules on enhanced antibacterial activity of biofunctionalaized silver nanoparticles. *Scientific Reports*, 10(1), 1–13. DOI: 10.1038/s41598-020-76726-7.

[68] Danaei, M., Dehghankhold, M., Ataei, S., Hasanzadeh Davarani, F., Javanmard, R., Dokhani, A., Khorasani, S., Mozafari, M.R. (2018). Impact of particle size and polydispersity index on the clinical applications of lipidic nanocarrier systems. *Pharmaceutics*, 10(2), 1–17. DOI: 10.3390/pharmaceutics10020057.

[69] Küp, F.Ö., Çoşkunçay, S., Duman, F. (2020). Biosynthesis of silver nanoparticles using leaf extract of Aesculus hippocastanum (horse chestnut): Evaluation of their antibacterial, antioxidant and drug release system activities. *Materials Science and Engineering C*, 107, 110207. DOI: 10.1016/j.msec.2019.110207.

[70] Edison, T.J.I., Sethuraman, M.G. (2012). Instant green synthesis of silver nanoparticles using Terminalia chebula fruit extract and evaluation of their catalytic activity on reduction of methylene blue. *Process Biochemistry*, 47(9), 1351–1357. DOI: 10.1016/j.procbio.2012.04.025.